Geochemical Perspectives Letters

Halogen enrichment on the continental surface: a perspective from loess

P.-Y. Han[1*], R.L. Rudnick[1], Z.-C. Hu[2], T. He[2], M.A.W. Marks[3], K. Chen[2]

OPEN ACCESS

https://doi.org/10.7185/geochemlet.2442

Abstract

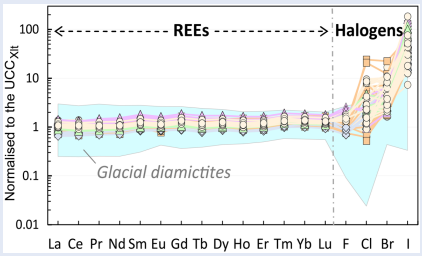

Halogen (F, Cl, Br, and I) concentrations for 129 loess samples from worldwide localities yield geometric means of 517 ± 53 µg/g F, 150 ± 20 µg/g Cl, 1.58 ± 0.16 µg/g Br, 1.16 ± 0.11 µg/g I (2 standard errors). These concentrations, notably for Br and I, are substantially higher than previous estimates for the average upper continental crystalline bedrocks, with enrichment factors of $1.3^{+0.7}_{-0.4}$ (F), $1.8^{+2.4}_{-0.8}$ (Cl), $3.8^{+1.3}_{-1.0}$ (Br), and 39^{+71}_{-16} (I) (95 % confidence), documenting enrichment of halogens on the continental surface. These surface halogens are likely sourced from the oceans and may be influenced by climate fluctuations. Halogen ratios (Br/Cl, I/Cl, and Br/I) in loess are similar to those of organic-rich soils/sediments from both terrigenous and marine settings, suggesting that terrigenous and marine organic matter have indistinguishable halogen ratios. The Br/I ratios differ from those in the fine grained matrix of glacial diamictites, indicating that another process (beyond biological influence) is responsible for fractionating halogens in the upper continental crust. Using a mixing model, we calculate that over 80–90 % of loess originates from crystalline bedrocks, while the remainder (<10–20 %) derives from the halogen- and organic-rich sedimentary cover or other sources (*e.g.*, marine aerosols).

Received 8 July 2024 | Accepted 2 October 2024 | Published 5 November 2024

Introduction

Halogens (F, Cl, Br, and I), an important group of lithophile and volatile elements, are primarily concentrated in Earth's surface reservoirs (*e.g.*, crust, seawater, and sediments) and play a critical role in modulating Earth's habitability (Kendrick, 2024 and references therein). To quantify the halogen cycle operating on Earth, it is necessary to have an accurate estimate of halogen distributions in different terrestrial reservoirs. However, such estimates are still lacking for much of the continental crust. This lack of knowledge regarding the geochemical behaviour of halogens during terrestrial geological processes, such as chemical weathering, metamorphic dehydration, and geobiological activity, limits our understanding of the role of the continental crust in the global halogen cycle, and also hinders our ability to utilise halogen concentrations and elemental ratios to trace geologic processes (Hanley and Koga, 2018).

To date, there are only five independent estimates of halogen concentrations in the upper continental crust (UCC), and these estimates can differ by up to a factor of ~50 (Shaw *et al.*, 1967; Wedepohl, 1995; Gao *et al.*, 1998; Muramatsu and Wedepohl, 1998; Han *et al.*, 2023). Poorly constrained halogen concentrations in continental rocks are partly due to heterogeneous halogen distributions, and partly due to the analytical challenges of obtaining precise and accurate halogen concentrations at low abundances, especially for Br and I. With recent advances in analytical techniques, Han *et al.* (2023) reported a comprehensive set of high quality F-Cl-Br-I data for 24 composite samples of the fine grained matrix of ancient glacial diamictites, considered a proxy for upper continental crust (Gaschnig *et al.*, 2016), and used these data to derive halogen estimates for the crystalline and weathered UCC. However, because the diamictites record chemical weathering in their provenance, the new estimates may represent minima for the crystalline UCC (Han *et al.*, 2023). Moreover, significant fractionation of Br/Cl and I/Cl ratios is observed in the glacial diamictites relative to pelagic sediments, and the reasons for this are unknown. These differences may reflect organic matter enrichment in the sea floor sediments relative to the UCC, chemical weathering of the UCC, or the effects of diagenesis/metamorphism on the diamictites (Han *et al.*, 2023). To better constrain the average halogen composition of the continental surface and to explore the mechanism(s) responsible for the fractionation of halogen ratios in sediments, we analysed 129 loess samples from worldwide localities.

Loess is a silt-sized, terrestrial aeolian sediment that covers about 10 % of the continental surface (Pye, 1995). Previous studies have used loess as a proxy for the average composition of the UCC because of its wide scale sampling of the continental surface, limited chemical weathering (compared to shales) and minor mineralogical and elemental fractionation during sedimentary transportation and deposition (*e.g.*, Taylor *et al.*, 1983; Gallet *et al.*, 1998; Chauvel *et al.*, 2014; Sauzéat *et al.*, 2015). However, previous research on loess mainly focused on

1. Department of Earth Science and Earth Research Institute, University of California - Santa Barbara, Santa Barbara, CA 93106, USA
2. State Key Laboratory of Geological Processes and Mineral Resources, China University of Geosciences, Wuhan, 430074, PR China
3. Eberhard Karls Universität Tübingen, Geo- und Umweltforschungszentrum, Schnarrenbergstraße 94-96, 72076 Tübingen, Germany
* Corresponding author (email: p_han@ucsb.edu)

insoluble elements like rare earth elements, with little attention paid to halogens. Only two previous studies have reported halogen concentrations in loess, each focusing on just one or two halogens (F and Cl by Liu *et al.*, 1981; I by Fan *et al.*, 2021) in loess-palaeosol profiles to track palaeoclimate. Thus, there have been no systematic studies of the behaviour of halogens in loess. Here, we report F-Cl-Br-I concentrations, along with major and rare earth element abundances, for 129 loess samples from Germany, Switzerland, the United States, Argentina, Kazakhstan, and China (Table S-1 and Fig. S-1), and discuss the behaviour of halogens on the continental surface and implications for global halogen recycling.

Halogen Concentrations and Mineralogical Hosts in Loess

Halogen concentrations were analysed by two methods: (1) combustion ion chromatography analysis (C-IC) for F, and (2) NH_4HF_2 digestion and ICPMS analysis (N-ICPMS) for Cl, Br, and I (Supplementary Information). Halogen concentrations of loess are reported in Table S-1 and plotted in Figure 1. Each halogen has distinctive geochemical properties, making each likely to be controlled by different phases in loess. Loess is mainly composed of quartz, feldspar, and various amounts of phyllosilicates and carbonates (Pye, 1995). Fluorine, with the smallest anionic radius of the group, may readily replace the hydroxyl anion and be incorporated into phyllosilicates. This is supported by a good correlation between F and Al_2O_3 ($R^2 = 0.84$) and K_2O ($R^2 = 0.78$) in loess, the latter two elements being enriched in phyllosilicates (Fig. 2a,b). Another mineral in loess capable of hosting F is carbonate, as two F^- can substitute for CO_3^{2-} (Feng *et al.*, 2021). However, F and CaO show a slight negative correlation (Fig. S-3), suggesting that F in loess is mainly controlled by phyllosilicates, rather than carbonates. The anti-correlation between F and CaO contrasts with the relatively high F content observed in some marine carbonates (Rude and Aller, 1991). The reason for a lack of carbonate control on F in the loess is unclear but may indicate that F substitution within carbonate occurs only in certain geological environments, which, in turn, might relate to the salinity, pCO_2, and/or temperature of the water body from which the carbonates precipitate (*e.g.*, Rude and Aller, 1991; Ramos *et al.*, 2005; Feng *et al.*, 2021).

The increasing anionic radii of Cl, Br, and I compared to F make them less likely to be incorporated into the crystal lattices of silicate minerals, particularly for Br and I. Instead, they may be absorbed on mineral surfaces or concentrated in fluid inclusions, evaporite minerals, and/or organic matter. We conducted a leaching experiment with MilliQ water on 14 samples to determine the location of these elements in loess (Table S-1 and Fig. S-4). The water soluble component of halogens in loess gradually decreases from Cl (as high as ~85 %) to Br (~50 %), to I (~25 %) (Fig. S-4), suggesting that most of the Cl in loess exists in soluble form, while Br and I are mainly present in water-insoluble phases. The soluble halogens in loess (Cl and Br) may originate from a range of sources: (1) soluble inorganic halogens incorporated or absorbed onto the silicate phases

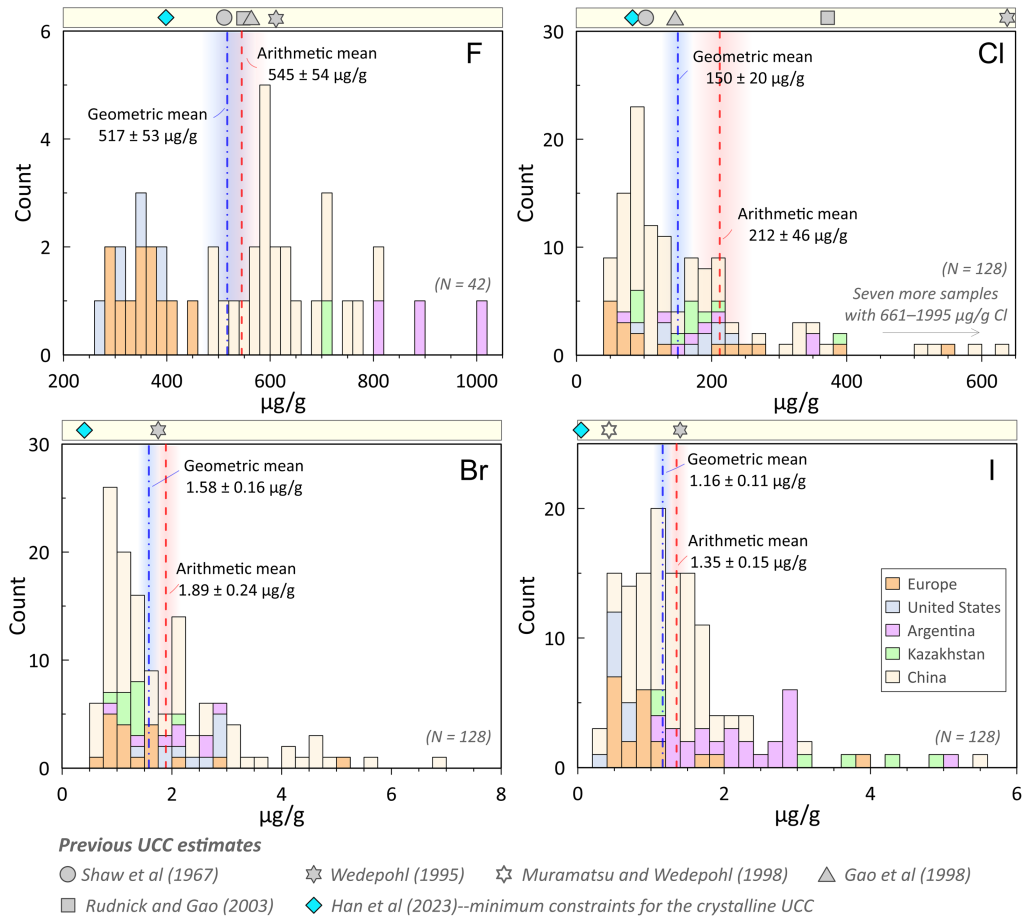

Figure 1 Halogen (F, Cl, Br, and I) concentrations of loess samples. The blue dash-dotted and the red dashed lines represent the geometric and arithmetic means of the loess data set, respectively, along with uncertainties of 2 standard errors (s.e., light-shaded bars; see Fig. S-5 for more details on the calculation). Symbols above each histogram represent previous estimates of halogen abundances in the UCC.

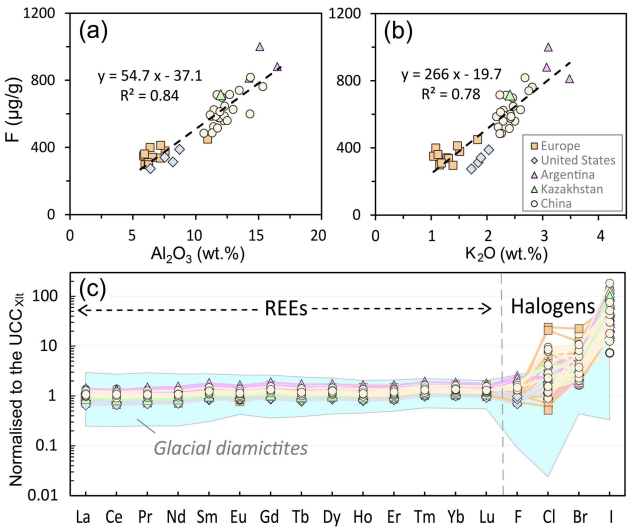

Figure 2 Fluorine *versus* **(a)** Al_2O_3 and **(b)** K_2O contents of loess. **(c)** Normalised rare earth element (REE) and halogen concentrations of loess samples relative to the composition of the crystalline UCC (UCC_{Xlt}): REE estimates for UCC are from Rudnick and Gao (2003) and halogens are from Han *et al.* (2023). The cyan-shaded area shows the compositional field of glacial diamictite composites.

within loess source materials, (2) soluble halogens in organic matter, (3) evaporite minerals like halite, and (4) post-depositional contamination from either anthropogenic sources and/or meteoric/ground water. The first three sources may reflect halogen distributions on the continental surface when loess deposits formed, while the fourth suggests potential disturbances of halogen contents after deposition. Since no significant regional differences are observed in the Cl and Br contents of samples from different areas (Fig. 1), and considering that their concentrations in meteoric water and groundwater are typically 10–100 times lower than those of loess (Worden, 2018), any enrichment from localised post-depositional processes, if they occurred, is likely minimal.

The concentrations of residual Br and I (after leaching) in loess are significantly higher than their averages in glacial diamictites (Fig. S-4). Because both elements have a strongly biophilic affinity, they may primarily be hosted in organic matter. Loess contains a significantly greater amount of organic matter than crystalline bedrocks, which are the main source of glacial diamictites (Han *et al.*, 2023). A possible reason for this difference might be the colder environment prevailing during the formation of glacial diamictites, leading to lower biomass on land surfaces and consequently less enrichment of halogens in the diamictites. This explanation also aligns with the proposition put forward by Fan *et al.* (2021) regarding climate fluctuations and I content in loess: in warmer periods, more halogens will be transported from the ocean to land and retained by surface biota, while during colder periods, both halogen transport efficiency and retention on land will decrease. In other words, halogen concentrations in terrigenous sediments, particularly for the less soluble Br and I, may be used as a proxy to monitor past temperature changes and to trace patterns of halogen movement between land and sea.

As a whole, the geometric and arithmetic means calculated from the data set are systematically higher than the recent estimates for crystalline UCC derived from data for ancient glacial diamictite composites (Han *et al.*, 2023). Using a bootstrap approach, we estimate the degree of halogen enrichment in loess relative to crystalline UCC to be $1.3^{+0.7}_{-0.4}$ times for F, $1.8^{+2.4}_{-0.8}$ times for Cl, $3.8^{+1.3}_{-1.0}$ times for Br, and 39^{+71}_{-16} times for I (95 % confidence, see Fig. S-6), with an exponential increase in enrichment from F to I (*i.e.* F < Cl < Br << I; Fig. 2c and Fig. S-7). There are two non-mutually exclusive factors that could explain the higher halogen contents in loess relative to glacial diamictites: (1) a lower degree of chemical weathering in the provenance of loess compared to that of glacial diamictites, and (2) greater potential for incorporation and preservation of organic matter in loess than in glacial diamictites (Fig. S-8). On the other hand, the mean halogen concentrations in loess are comparable to previous estimates of halogens in the UCC based on either large scale sampling (Shaw *et al.*, 1967; Gao *et al.*, 1998) or models based on lithologies (Wedepohl, 1995; Muramatsu and Wedepohl, 1998) (Fig. 1), both of which incorporate data not only for crystalline bedrocks, but also for many halogen-rich lithologies such as shales, carbonates, and evaporites from the overlying sedimentary cover. The similarity between mean halogen concentrations in loess and these previous estimates suggests that halogens in loess may provide a useful average of halogen concentrations across various types of rocks and sediments at the continental surface. Halogen enrichment on the continental surface may derive from the oceans, a major halogen reservoir (Hanley and Koga, 2018), with halogen fluxes from oceans to continents potentially regulated by climate fluctuations, as suggested by Fan *et al.* (2021).

Halogen Ratios in Loess

The Br/Cl and I/Cl ratios of loess, as well as the leached residues of loess samples, are significantly fractionated relative to those in igneous rocks like MORB/OIB and arc/backarc lavas, closely tracking the compositional range seen in pelagic sediments, whose halogen concentrations are primarily controlled by marine organic matter (John *et al.*, 2011) (Fig. 3). This supports the inference above, based on leaching experiments (Fig. S-4), that Br and I primarily reside in water-insoluble organic matter in loess. It also suggests that both terrigenous and marine organic matter have indistinguishable halogen ratios. This notion is further supported by the consistently narrow range of the Br/I ratio observed in organic-rich soils and sediments from Japan (Yamasaki *et al.*, 2015) and China (He *et al.*, 2018) (Fig. S-9). However, no correlation is observed between Br (or I) and TOC in either the loess or Japanese soil samples (Fig. S-10), which is somewhat counterintuitive and may result from varying Br/TOC (or I/TOC) ratios in different types of organic matter (Muramatsu and Wedepohl, 1998; Mayer *et al.*, 2007). Therefore, great caution should be exercised when using the correlation of Br and I with TOC to infer the presence of organohalogens in sediments.

The halogen ratios observed in loess are also similar to those found in blueschists and serpentinites from subduction zone settings (Fig. 3), indicating that the halogens in these metamorphic rocks may be overprinted by fluids derived from subducted terrigenous organic-bearing sediments, not just marine sediments (*e.g.*, John *et al.*, 2011; Kendrick *et al.*, 2013; Pagé *et al.*, 2016). Most glacial diamictite composites (excluding five carbonate and terrigenous sediment-rich samples from Namibia), however, have significantly higher Br/I ratios (7–74) compared to loess (0.25–6.3) (Fig. 3). This difference suggests that halogen ratios are significantly fractionated within the upper continental crust by an additional process, such as continental weathering and/or diagenesis/metamorphism. We note that the diamictites generally carry a stronger chemical weathering signature than loess (Fig. S-8), and most experienced greenschist facies metamorphism (Han *et al.*, 2023).

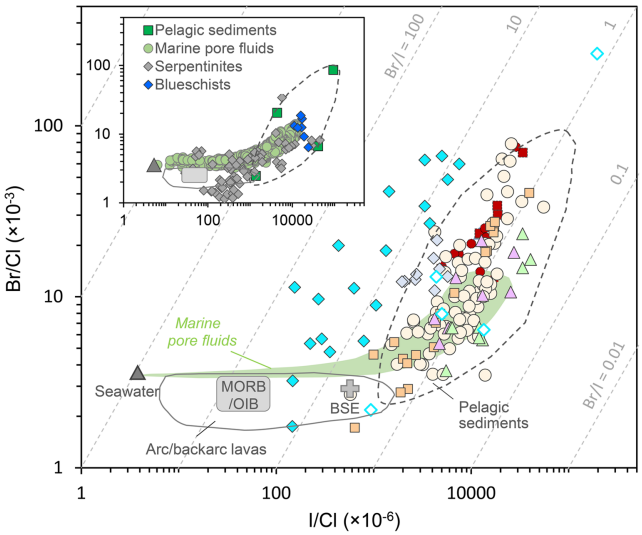

Figure 3 Br/Cl *versus* I/Cl ratios of loess (symbols as in Fig. 2; this study) and glacial diamictite composites (cyan diamonds; Han *et al.*, 2023). Note that (1) the leached loess residues are plotted as deep-red dashed symbols, and (2) five carbonate-rich and terrigenous sediment-rich glacial diamictites from Namibia have notably elevated I content and relatively low Br/I ratios and are shown with open diamonds (see Han *et al.*, 2023 for discussion). Halogen ratios of seawater (grey triangle), bulk silicate Earth (BSE, grey plus sign), mid-ocean ridge and ocean island basalts (MORB/OIB, grey rectangle, Kendrick *et al.*, 2017), arc/backarc lavas (grey outline, Kendrick *et al.*, 2020), pelagic sediments (grey dashed outline, John *et al.*, 2011), and marine pore fluids (green field, Fehn *et al.*, 2006; Muramatsu *et al.*, 2007) are plotted for comparison. Thin grey dashed lines are constant Br/I ratio contours, ranging from 0.01 to 10,000. The inset shows samples from the subduction zone setting: pelagic sediments, marine pore fluids, serpentinites (John *et al.*, 2011; Kendrick *et al.*, 2013), and blueschists (Pagé *et al.*, 2016).

Implications for Loess Provenance

Previous studies suggested that loess derives from rocks that have generally experienced moderate chemical weathering during multiple cycles of sedimentation (Gallet *et al.*, 1998; Sauzéat *et al.*, 2015). Based on the Li isotopic composition of loess, Sauzéat *et al.* (2015) estimated that the proportion of chemically weathered material at Earth's surface was 37^{+17}_{-10} %. However, because Li isotopes are not sensitive to the presence of organic matter, it remains unclear what proportion of material within loess is derived from pulverised unweathered crystalline bedrocks *versus* mature sediments that have extensively interacted with the biosphere. As Br and I are strongly enriched in organic-bearing sediments and their concentrations will be sensitive to the amount of such sediment in the loess provenance; we used a mixing model to calculate the proportions of the above sources in loess. In this calculation, the Br and I contents in loess are assumed to result from a mixture of (1) clastic sediments derived from glacially pulverised unweathered crystalline bedrocks, (2) an overlying halogen-rich sedimentary cover, and (3) inputs from other sources, such as precipitation (marine aerosols) and evaporite minerals (Fig. 4). Although the composition of the third end member is difficult to define and may vary between samples and locations, we assume that the first end member is well represented by the glacial diamictites (Han *et al.*, 2023), and the second by the Japanese soil samples (Yamasaki *et al.*, 2015). When projecting the geometric or arithmetic mean of Japanese soils (Fig. S-11) onto the mixing line for either Br or I, assuming no other inputs, the calculated mass proportions of the UCC crystalline bedrocks in loess are consistently >80–90 % (Fig. 4). This proportion would be even higher if other inputs were considered. Overall, this suggests that the sediments that have extensively interacted with the biosphere in the loess provenance is <10–20 %, which is somewhat lower than the sum proportion of chemically weathered components, 37^{+17}_{-10} %, at

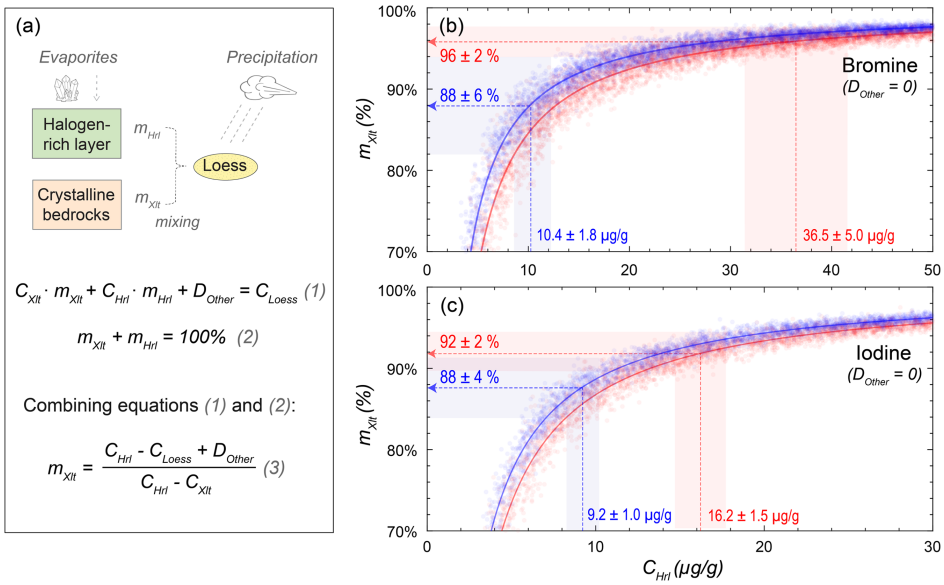

Figure 4 **(a)** Mixing model for the source of halogens in loess. In the equations, C_{Xlt}, C_{Hrl}, and C_{Loess} represent halogen concentrations of the UCC crystalline bedrocks, halogen-rich sedimentary layer, and loess, respectively; D_{Other} represents other potential inputs from precipitation and/or evaporites that could contribute significant halogens without substantially affecting the system's mass; m_{Xlt} and m_{Hrl} are assumed mass proportions of the UCC crystalline bedrocks and the sedimentary halogen-rich component in loess. **(b)** and **(c)** show the simulated relationship between m_{Xlt} and C_{Hrl} from Equation 3 in **(a)** when $D_{Other} = 0$, for mixing of Br and I, respectively. The red and blue curves are calculated using either the geometric (blue) or arithmetic (red) means of the loess samples and the adjacent pale red/blue circles represent related errors (modelled from Monte Carlo re-sampling; 10,000 times). The vertical dashed lines are geometric (in blue, 2 s.e.) and arithmetic (in red, 2 s.e.) means of Japanese soils. The calculated mass proportion of crystalline rocks in loess is shown as horizontal dashed lines (with 2σ uncertainties), which are obtained when projecting the geometric or arithmetic mean of Japanese soils (Fig. S-10) to the red or blue curves.

the continental surface as estimated by Sauzéat *et al.* (2015). Thus, it can be concluded that the primary source of loess material is the crystalline bedrocks of the UCC, which validates its use to infer the average composition of the present day UCC (Taylor *et al.*, 1983; Gallet *et al.*, 1998; Chauvel *et al.*, 2014).

Acknowledgements

We dedicate this to the memory of Prof. Shan Gao (1962-2016), who influenced so much of our work on crust composition. We thank Hui Cao and Lang Wang for assistance with the N-ICPMS analyses, Gabriele Stoschek for help with the C-IC analyses, and Shin-ichi Yamasaki for providing the Japanese soil data. This work was supported by the State Key Laboratory of Geological Processes and Mineral Resources (GPMR202204), the University of California at Santa Barbara, and the U.S. National Science Foundation (EAR2321367). TH acknowledges the support from the National Natural Science Foundation of China (42103031). We are grateful to Romain Tartèse, Mark A. Kendrick, and two anonymous reviewers for constructive comments that helped us to improve the manuscript.

Editor: Romain Tartèse

Additional Information

Supplementary Information accompanies this letter at https://www.geochemicalperspectivesletters.org/article2442.

Cite this letter as: Han, P.-Y., Rudnick, R.L., Hu, Z.-C., He, T., Marks, M.A.W., Chen, K. (2024) Halogen enrichment on the continental surface: a perspective from loess. *Geochem. Persp. Let.* 32, 52–57. https://doi.org/10.7185/geochemlet.2442

References

Chauvel, C., Garçon, M., Bureau, S., Besnault, A., Jahn, B.-m., Ding, Z. (2014) Constraints from loess on the Hf–Nd isotopic composition of the upper continental crust. *Earth and Planetary Science Letters* 388, 48–58. https://doi.org/10.1016/j.epsl.2013.11.045

Fan, Y., Zhou, W., Hou, X., Kong, X., Chen, N., Burr, G.S. (2021) Indication of new climatic proxy by loess iodine variation. *Quaternary Science Reviews* 251, 106720. https://doi.org/10.1016/j.quascirev.2020.106720

Fehn, U., Lu, Z., Tomaru, H. (2006) Data report: ^{129}I/I ratios and halogen concentrations in pore water of Hydrate Ridge and their relevance for the origin of gas hydrates: A progress report. In: Tréhu, A.M., Bohrmann, G., Torres, M.E., Colwell, F.S. (Eds.) *Proceedings of the Ocean Drilling Program: Scientific Results Volume 204*. Texas A & M University, College Station, TX. 1–25. https://doi.org/10.2973/odp.proc.sr.204.107.2006

Feng, X., Steiner, Z., Redfern, S.A. (2021) Fluorine incorporation into calcite, aragonite and vaterite $CaCO_3$: Computational chemistry insights and geochemistry implications. *Geochimica et Cosmochimica Acta* 308, 384–392. https://doi.org/10.1016/j.gca.2021.05.029

Gallet, S., Jahn, B.-m., Lanoë, B.V.V., Dia, A., Rossello, E. (1998) Loess geochemistry and its implications for particle origin and composition of the upper continental crust. *Earth and Planetary Science Letters* 156, 157–172. https://doi.org/10.1016/S0012-821X(97)00218-5

Gao, S., Luo, T.C., Zhang, B.R., Zhang, H.F., Han, Y.W., Zhao, Z.D., Hu, Y.K. (1998) Chemical composition of the continental crust as revealed by studies in East China. *Geochimica et Cosmochimica Acta* 62, 1959–1975. http://dx.doi.org/10.1016/S0016-7037(98)00121-5

Gaschnig, R.M., Rudnick, R.L., McDonough, W.F., Kaufman, A.J., Valley, J.W., Hu, Z., Gao, S., Beck, M.L. (2016) Compositional of the upper continental crust through time, as constrained by ancient glacial diamictites. *Geochimica et Cosmochimica Acta* 186, 316–343. https://doi.org/10.1016/j.gca.2016.03.020

Han, P.-Y., Rudnick, R.L., He, T., Marks, M.A., Wang, S.-J., Gaschnig, R.M., Hu, Z.-C. (2023) Halogen (F, Cl, Br, and I) concentrations of the upper continental crust through time as recorded in ancient glacial diamictite composites. *Geochimica et Cosmochimica Acta* 341, 28–45. https://doi.org/10.1016/j.gca.2022.11.012

Hanley, J.J., Koga, K.T. (2018) Halogens in terrestrial and cosmic geochemical systems: abundances, geochemical behaviors, and analytical methods. In: Harlov, D., Aranovich, L. (Eds.) *The role of halogens in Terrestrial and Extraterrestrial Geochemical Processes*. Springer, Cham. 21–121. https://doi.org/10.1007/978-3-319-61667-4_2

He, T., Xie, J., Hu, Z., Liu, T., Zhang, W., Chen, H., Liu, Y., Zong, K., Li, M. (2018) A rapid acid digestion technique for the simultaneous determination of bromine and iodine in fifty-three Chinese soils and sediments by ICP-MS. *Geostandards and Geoanalytical Research* 42, 309–318. https://doi.org/10.1111/ggr.12212

John, T., Scambelluri, M., Frische, M., Barnes, J.D., Bach, W. (2011) Dehydration of subducting serpentinite: implications for halogen mobility in subduction zones and the deep halogen cycle. *Earth and Planetary Science Letters* 308, 65–76. https://doi.org/10.1016/j.epsl.2011.05.038

Kendrick, M.A. (2024) Halogen Cycling in the Solid Earth. *Annual Review of Earth and Planetary Sciences* 52. https://doi.org/10.1146/annurev-earth-031621-111700

Kendrick, M.A., Honda, M., Pettke, T., Scambelluri, M., Phillips, D., Giuliani, A. (2013) Subduction zone fluxes of halogens and noble gases in seafloor and forearc serpentinites. *Earth and Planetary Science Letters* 365, 86–96. https://doi.org/10.1016/j.epsl.2013.01.006

Kendrick, M., Hémond, C., Kamenetsky, V., Danyushevsky, L., Devey, C.W., Rodemann, T., Jackson, M., Perfit, M. (2017) Seawater cycled throughout Earth's mantle in partially serpentinized lithosphere. *Nature Geoscience* 10, 222–228. https://doi.org/10.1038/ngeo2902

Kendrick, M.A., Danyushevsky, L.V., Falloon, T.J., Woodhead, J.D., Arculus, R.J., Ireland, T. (2020) SW Pacific arc and backarc lavas and the role of slab-bend serpentinites in the global halogen cycle. *Earth and Planetary Science Letters* 530, 115921. https://doi.org/10.1016/j.epsl.2019.115921

Liu, Y., Wen, Q., Chen, Q. (1981) F/Cl ratio in Luochuan loess section, Shaanxi province—A geochemical index for paleoclimatic fluctuation. *Geochimica*, 388–391

Mayer, L.M., Schick, L.L., Allison, M.A., Ruttenberg, K.C., Bentley, S.J. (2007) Marine vs. terrigenous organic matter in Louisiana coastal sediments: The uses of bromine: organic carbon ratios. *Marine Chemistry* 107, 244–254. https://doi.org/10.1016/j.marchem.2007.07.007

Muramatsu, Y., Wedepohl, K.H. (1998) The distribution of iodine in the earth's crust. *Chemical Geology* 147, 201–216. https://doi.org/10.1016/S0009-2541(98)00013-8

Muramatsu, Y., Doi, T., Tomaru, H., Fehn, U., Takeuchi, R., Matsumoto, R. (2007) Halogen concentrations in pore waters and sediments of the Nankai Trough, Japan: Implications for the origin of gas hydrates. *Applied Geochemistry* 22, 534–556. https://doi.org/10.1016/j.apgeochem.2006.12.015

Pagé, L., Hattori, K., de Hoog, J.C., Okay, A.I. (2016) Halogen (F, Cl, Br, I) behaviour in subducting slabs: A study of lawsonite blueschists in western Turkey. *Earth and Planetary Science Letters* 442, 133–142. https://doi.org/10.1016/j.epsl.2016.02.054

Pye, K. (1995) The nature, origin and accumulation of loess. *Quaternary Science Reviews* 14, 653–667. https://doi.org/10.1016/0277-3791(95)00047-X

Ramos, A., Ohde, S., Hossain, M., Ozaki, H., Sirirattanachai, S., Apurado, J. (2005) Determination of fluorine in coral skeletons by instrumental neutron activation analysis. *Journal of radioanalytical and nuclear chemistry* 266, 19–29. https://doi.org/10.1007/s10967-005-0863-x

Rude, P.D., Aller, R.C. (1991) Fluorine mobility during early diagenesis of carbonate sediment: An indicator of mineral transformations. *Geochimica et Cosmochimica Acta* 55, 2491–2509. https://doi.org/10.1016/0016-7037(91)90368-F

Rudnick, R.L., Gao, S. (2003) Composition of the Continental Crust. *Treatise on Geochemistry*, 1–64. https://doi.org/10.1016/B0-08-043751-6/03016-4

Sauzéat, L., Rudnick, R.L., Chauvel, C., Garçon, M., Tang, M. (2015) New perspectives on the Li isotopic composition of the upper continental crust and its

weathering signature. *Earth and Planetary Science Letters* 428, 181–192. https://doi.org/10.1016/j.epsl.2015.07.032

Shaw, D., Reilly, G., Muysson, J., Pattenden, G., Campbell, F. (1967) An Estimate of the Composition of the Canadian Precambrian shield. *Canadian Journal of Earth Sciences* 4, 829–853. https://doi.org/10.1139/e67-058

Taylor, S.R., Mclennan, S.M., McCulloch, M.T. (1983) Geochemistry of loess, continental crustal composition and crustal model ages. *Geochimica et Cosmochimica Acta* 47, 1897–1905. https://doi.org/10.1016/0016-7037(83)90206-5

Wedepohl, K.H. (1995) The composition of the continental crust. *Geochimica et Cosmochimica Acta* 59, 1217–1232. https://doi.org/10.1016/0016-7037(95)00038-2

Worden, R.H. (2018) Halogen Elements in Sedimentary Systems and Their Evolution During Diagenesis. In: Harlov, D., Aranovich, L. (Eds.) *The Role of Halogens in Terrestrial and Extraterrestrial Geochemical Processes*. Springer, Cham. 185–260. https://doi.org/10.1007/978-3-319-61667-4_4

Yamasaki, S.-i., Takeda, A., Watanabe, T., Tagami, K., Uchida, S., Takata, H., Maejima, Y., Kihou, N., Tsuchiya, N. (2015) Bromine and iodine in Japanese soils determined with polarizing energy dispersive X-ray fluorescence spectrometry. *Soil Science and Plant Nutrition* 61, 751–760. https://doi.org/10.1080/00380768.2015.1054773

Geochemical Perspectives Letters

Halogen enrichment on the continental surface: a perspective from loess

P-Y. Han, R.L. Rudnick, Z-C. Hu, T. He, M.A. Marks, K. Chen

Supplementary Information

The Supplementary Information includes:

- Samples and Analytical Methods
- Tables S-1
- Figures S-1 to S-11
- Supplementary Information References

Samples and Analytical Methods

The 129 loess samples investigated in this study were collected from four continents: Europe (Germany and Switzerland), North America (United States), South America (Argentina), and Asia (Kazakhstan and China). The latitude and longitude of the loess sections, along with references to the original investigations of these units, are given in Table S-1 and plotted in Figure S-1. Data for major elements, rare earth elements (REEs), total organic carbon (TOC), and halogens are reported in this study.

Major Elements and REE Analyses

The samples were powdered in an agate mortar mill (RS200, Retsch, Germany) prior to analysis. Major element concentrations were determined by X-ray fluorescence (RIX2100, Japan) on fused glass disks at Northwest University in Xi'an, China. Reference materials BCR-2 (basalt, USGS) and GSR-3 (basalt, Chinese National Standard) indicate that precision and accuracy are better than 5 %. Rare earth elements were analysed by ICP-MS (Agilent 7900) after high-pressure acid digestion of samples in Teflon bombs at the State Key Laboratory of Geological Processes and Mineral Resources (GPMR), China University of Geosciences, Wuhan. About 50 mg of sample powder was weighed into a Teflon bomb, and then 1 ml of concentrated HNO_3 and 1 ml of concentrated HF were added. The sealed bomb was heated at 190 °C in the oven for 72 hours. After cooling, the solution was evaporated to dryness at ~120 °C. This was followed by adding 1 ml of concentrated HNO_3 and evaporating to dryness again. The resultant salt was re-dissolved by adding 1 ml of HNO_3, 1 ml of Milli-Q water (18.2 MΩ), and 1 ml of 1µg/ml In internal standard solution. The solution was then resealed and heated in the bomb at 190 °C for ~24 hours. The final solution was diluted to ~100 g with 2 %

HNO_3 for ICP-MS analysis. Total procedure blanks are below detection limits. The results for reference materials (BCR-2, BHVO-2, AGV-2, and SCo-1) agree well with the recommended values, within 10 % uncertainties. Results for the reference materials are in Park *et al.* (2012).

Total Organic Carbon Analysis

Organic C measurements were conducted at the State Key Laboratory of Biogeology and Environmental Geology, China University of Geosciences, Wuhan. About 2 g of powdered sample was acidified with 50 % HCl to remove inorganic carbon from carbonates. The residue was rinsed with deionised water to neutralise pH, then centrifuged and dried for 48 hours, before being analysed using the 902 T C–S analyser (Beijing Wanliandaxinke Instruments Co. Ltd.). Based on multiple analyses of AR-4007 (total carbon: 7.62 %, Alpha Resources Inc.), AR-4017 (total carbon: 0.50 ± 0.03 %, Alpha Resources Inc.) and B2152 (total carbon: 1.30 ± 0.09 %, Elemental Microanalysis Ltd.), TOC data are reported with a precision better than ± 0.1 %.

Halogen Analyses and Leaching Experiment

Halogen concentrations of loess are obtained using two different methods: (1) F-Cl-Br analysis by combustion ion chromatography analysis (C-IC) conducted at Fachbereich Geowissenschaften, Universität Tübingen, and (2) Cl-Br-I analysis by NH_4HF_2 digestion and ICPMS analysis (N-ICPMS) conducted at State Key Laboratory of Geological Processes and Mineral Resources, China University of Geosciences, Wuhan. More detailed descriptions of these two methods can be found in Han *et al*. (2023). Although Cl and Br are both analysed in the above two methods, the measured Cl and Br content in loess by C-IC are often 25-50 % lower than those obtained by N-ICPMS, which is consistent with the results obtained by Han *et al*. (2023) on glacial diamictites (Fig. S-2). This discrepancy could result from incomplete halogen recovery by pyrohydrolysis (*e.g.*, Marks *et al*., 2017; Kendrick *et al*., 2018; Han *et al*., 2023). Therefore, we used the F data from C-IC and the Cl, Br, I data from N-ICPMS in this paper to investigate the behaviour of halogens in loess (Table S-1 and Fig. 1).

Halogen leaching experiments were performed on 14 loess samples from various localities (five from Germany, one from the United States, one from Kazakhstan, and seven from China) at State Key Laboratory of Geological Processes and Mineral Resources, China University of Geosciences, Wuhan. For each sample, ~150 mg of sample powder was first mixed with 5 ml Milli-Q water (18.2 MΩ), then sonicated for 5 minutes using ultrasound, and subsequently centrifuged for 7 minutes in a centrifuge. The solid residue was then separated and dried in an oven at 50 ºC for 48 hours. Finally, the residual sample powders were dissolved and analysed for Cl-Br-I content using the above N-ICPMS method.

Supplementary Table

Table S-1 Major elements, total organic carbon (TOC), and rare earth elements of loess samples.

Table S-1 is available for download (.xlsx) from the online version of this article at https://doi.org/10.7185/geochemlet.2442.

Supplementary Figures

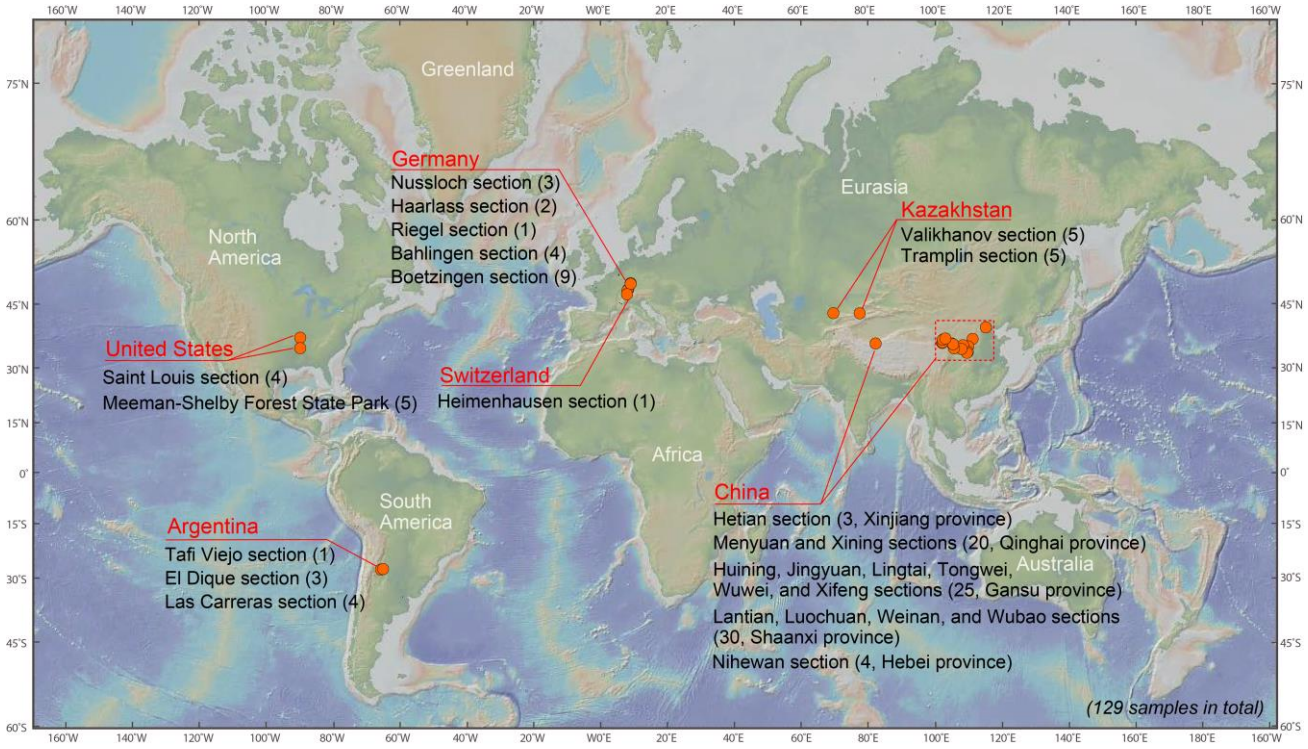

Figure S-1 Distribution of loess samples from this study. The number in parentheses indicates the quantity of samples analysed in each section.

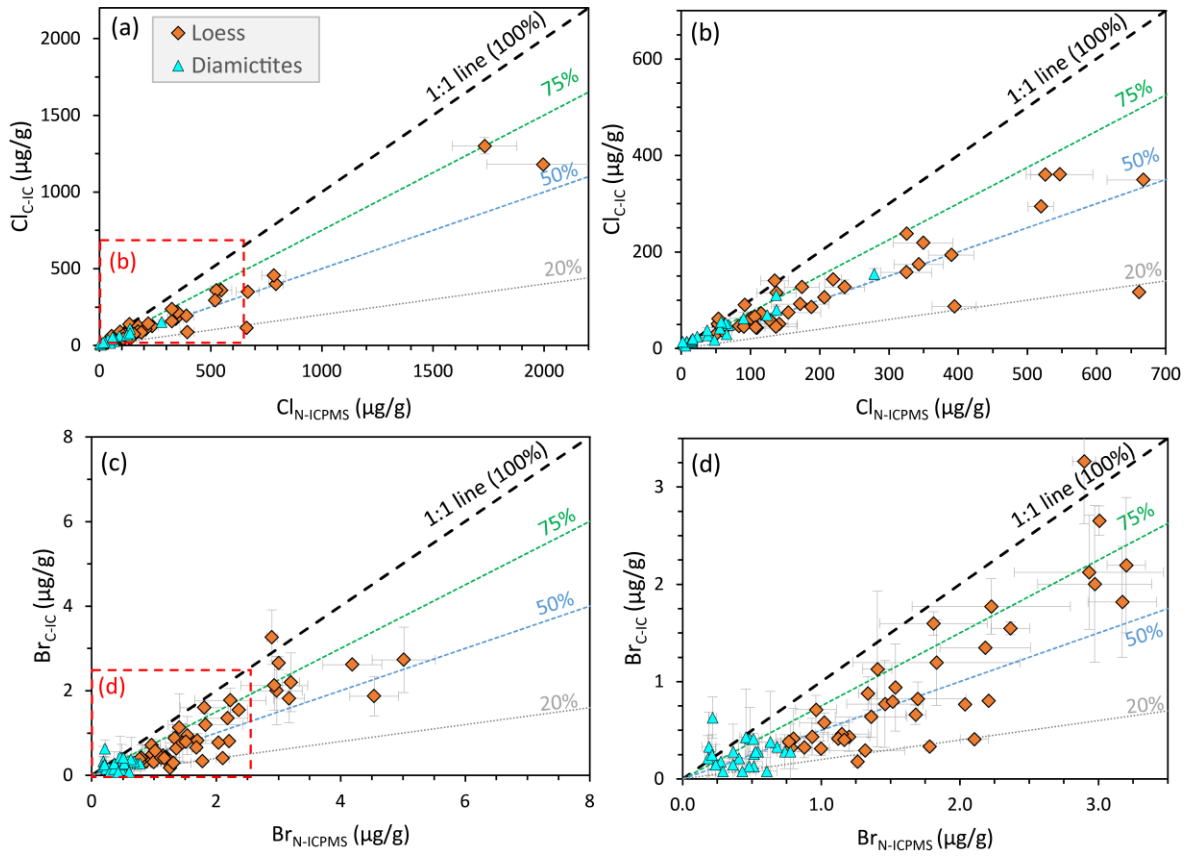

Figure S-2 Comparison of Cl **(a-b)** and Br **(c-d)** results for loess (this study) and glacial diamictite composites (Han *et al*., 2023) by C-IC and N-ICPMS, respectively. Error bars represent 1σ.

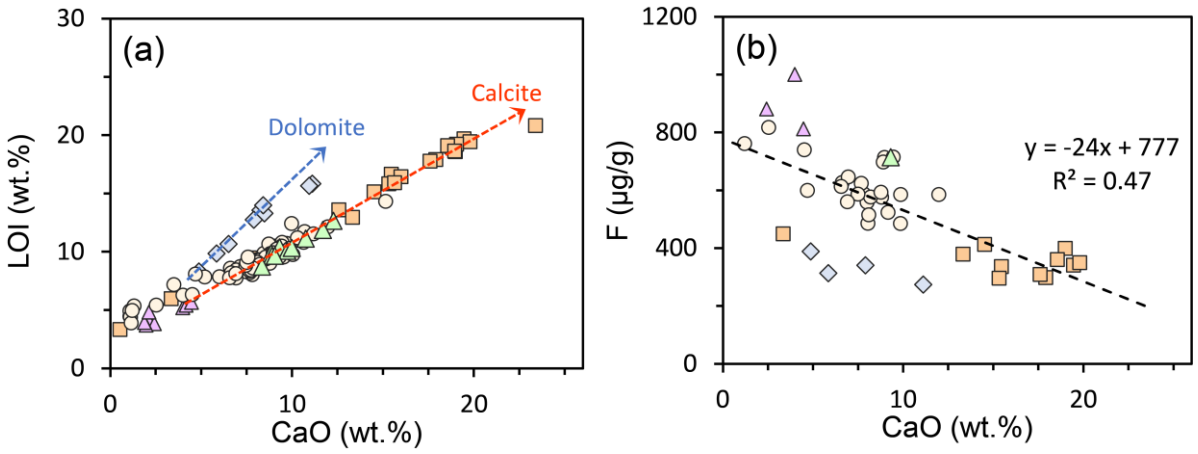

Figure S-3 **(a)** Loss of Ignition (LOI) of loess increases as the CaO content increases. The data follow the trends produced by having variable amounts of calcite (red-dashed line) and dolomite (blue dashed line) in the samples, suggesting that the CaO in loess is mainly controlled by carbonate. **(b)** Fluorine versus CaO content. There is a negative trend between F and CaO, likely due to the dilution of F content in loess samples by carbonate. Symbols as Fig. 2.

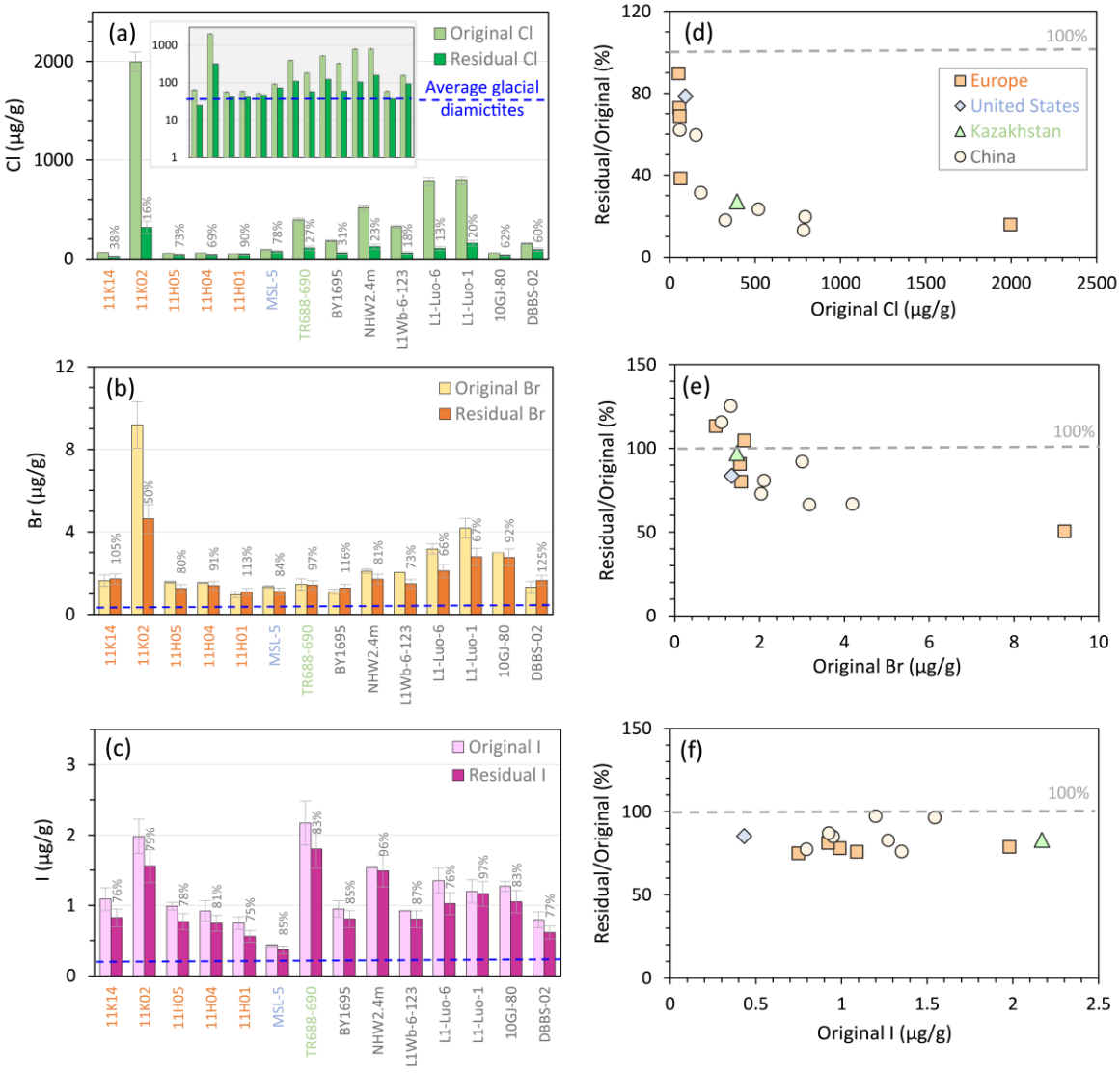

Figure S-4 Leaching experiments on loess samples for Cl, Br, and I. **(a-c)** show the Cl, Br, and I contents of the samples (on the x-axis) both before (original) and after (residual) leaching. The blue dashed lines represent the average Cl-Br-I content of glacial diamictites from Han et al. (2023). The inset figure in **(a)** is in log-scale. In **(d-f)**, the proportion of residual halogen components in the analysed loess samples (y-axis) is plotted against the original halogen concentrations (x-axis).

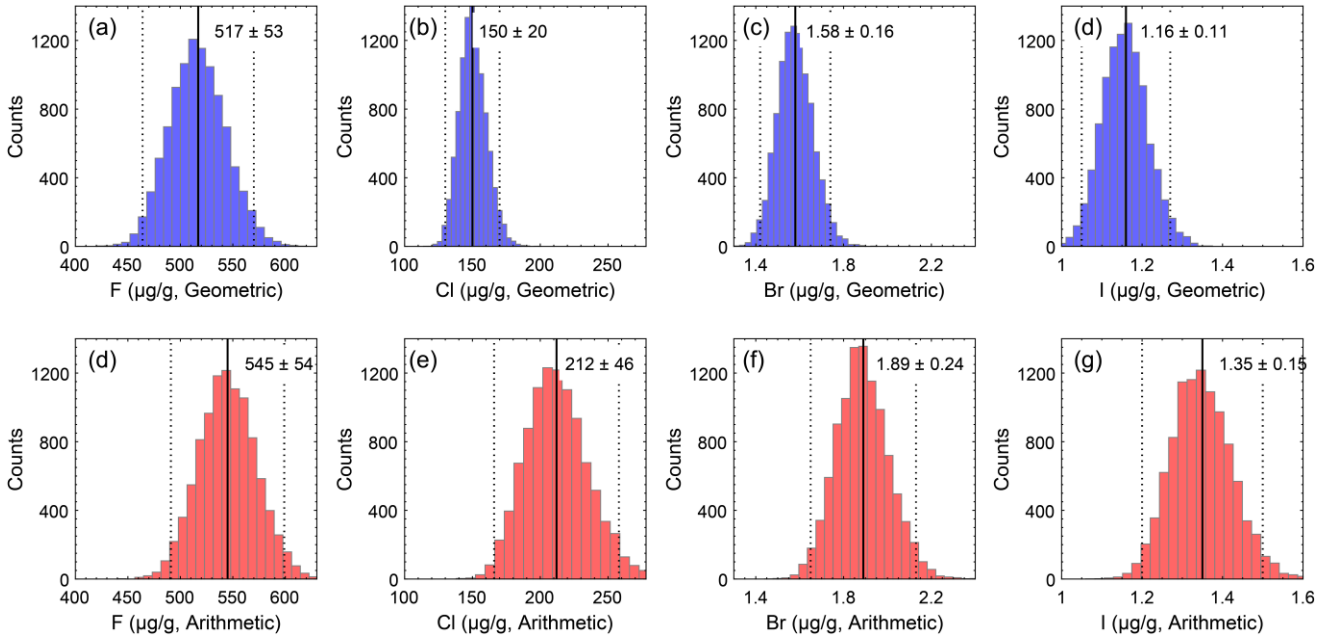

Figure S-5 Bootstrapped geometric **(a-d**, upper panel**)** and arithmetic **(d-g**, lower panel**)** means of loess F-Cl-Br-I data, which are computed using MATLAB, employing 10,000 trials. Each trial represents the geometric or arithmetic mean of a randomly resampled set of the loess data, with replacement allowed. The geometric/arithmetic means for the loess samples (Fig. 1) are determined by averaging the results of the 10,000 bootstrapped trials, shown as vertical black lines (2 standard errors indicated by black dashed lines). The arithmetic means consistently surpass the geometric means due to the skewed distribution of halogen concentrations in loess (Fig. 1).

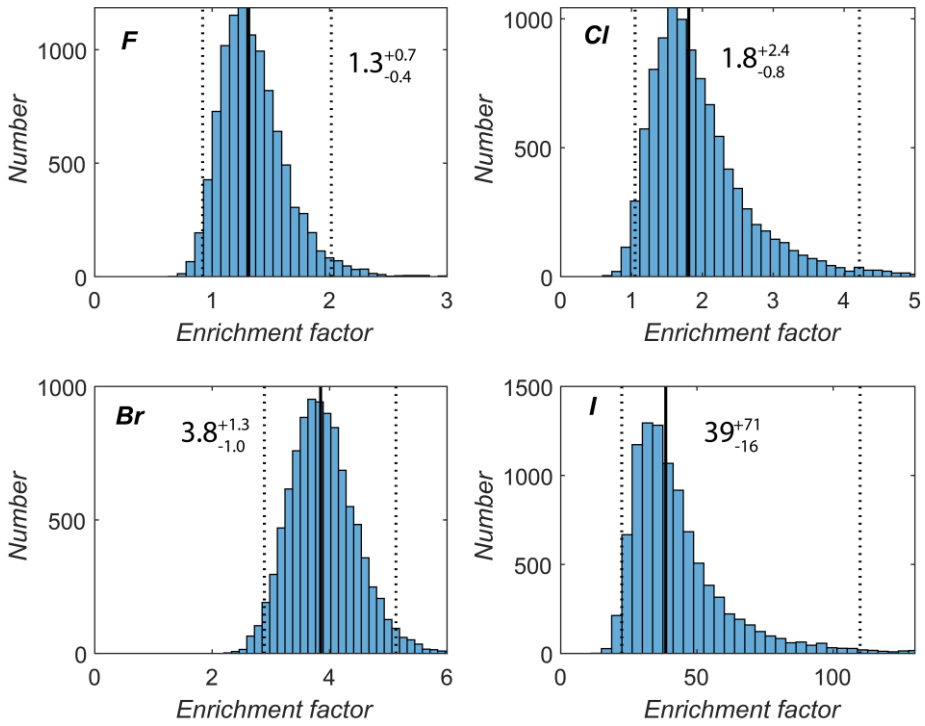

Figure S-6 Enrichment factor of halogens in loess relative to the estimates of the crystalline UCC (394 ± 67 µg/g F, 83 ± 24 µg/g Cl, 0.41 ± 0.04 µg/g Br, and 0.03 ± 0.01 µg/g I, with 2 standard deviations, from Han *et al.*, 2023), calculated by bootstrapping, with 10,000 trials. Each trial represents the median of randomly sampled loess compared to a random composition of the crystalline UCC within its 2 standard deviations. The black line represents the median of the 10,000 bootstrapped trials, and the dashed lines are 95 % confidence interval.

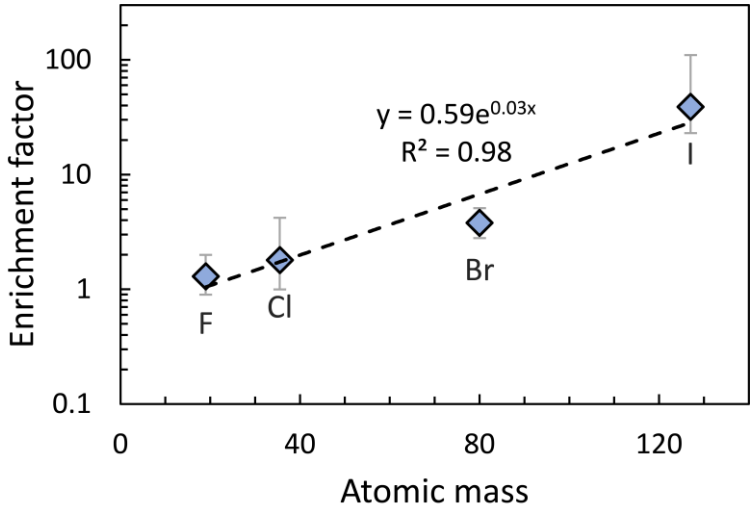

Figure S-7 The halogen enrichment factors in loess increase exponentially with their atomic masses. Error bars of halogen enrichment factors are at 95 % confidence level, see Figure S-6 for further details.

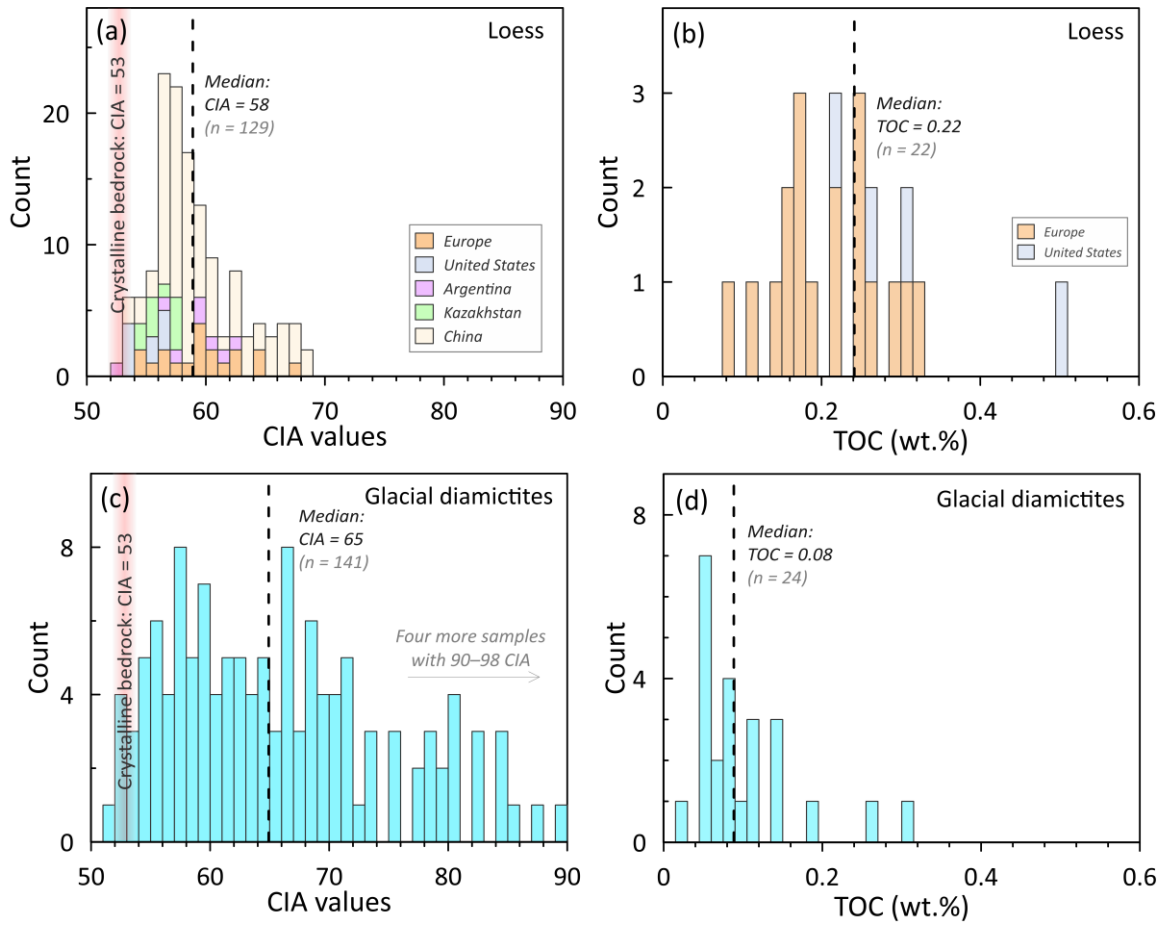

Figure S-8 Comparison of CIA value (chemical index of alteration, CIA = molar Al_2O_3 / (Al_2O_3 + CaO^*+ K_2O + Na_2O), where CaO^* is corrected for carbonate and apatite (Nesbitt and Young, 1982) and the carbonate correction is based on the approach of McLennan (1993), **a** and **c)** and TOC results **(b** and **d)** for loess (this study) and glacial diamictite composites, respectively. The CIA values of glacial diamictites are from Gaschnig *et al.* (2016) for 141 individual glacial diamictite samples, and the TOC data are from Greaney *et al.* (2020) for 24 glacial diamictite composites. The dashed line in each plot represents the median value for each population, and loess samples generally have limited and lower CIA values but higher TOC than glacial diamictites.

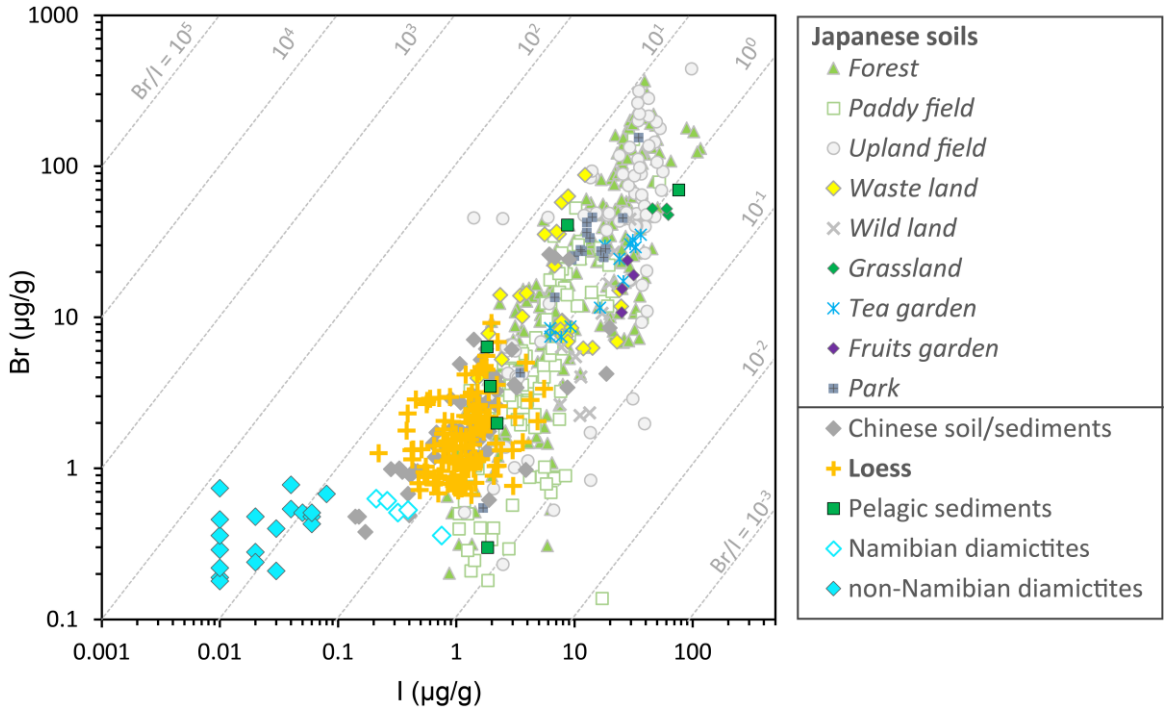

Figure S-9 Br versus I content of Japanese soils (Yamasaki *et al.*, 2015), Chinese soils/sediments (He *et al*., 2018), loess (this study), pelagic sediments (John *et al*., 2011), and glacial diamictites (Han et al., 2023). Within the glacial diamictite composites, five samples from Namibia exhibit notably elevated I content and relatively low Br/I ratios (the elevated I content of the Namibian samples is likely due to the presence of carbonate and abundant terrigenous sedimentary rocks in their provenance, see discussion in Han *et al*. (2023)).

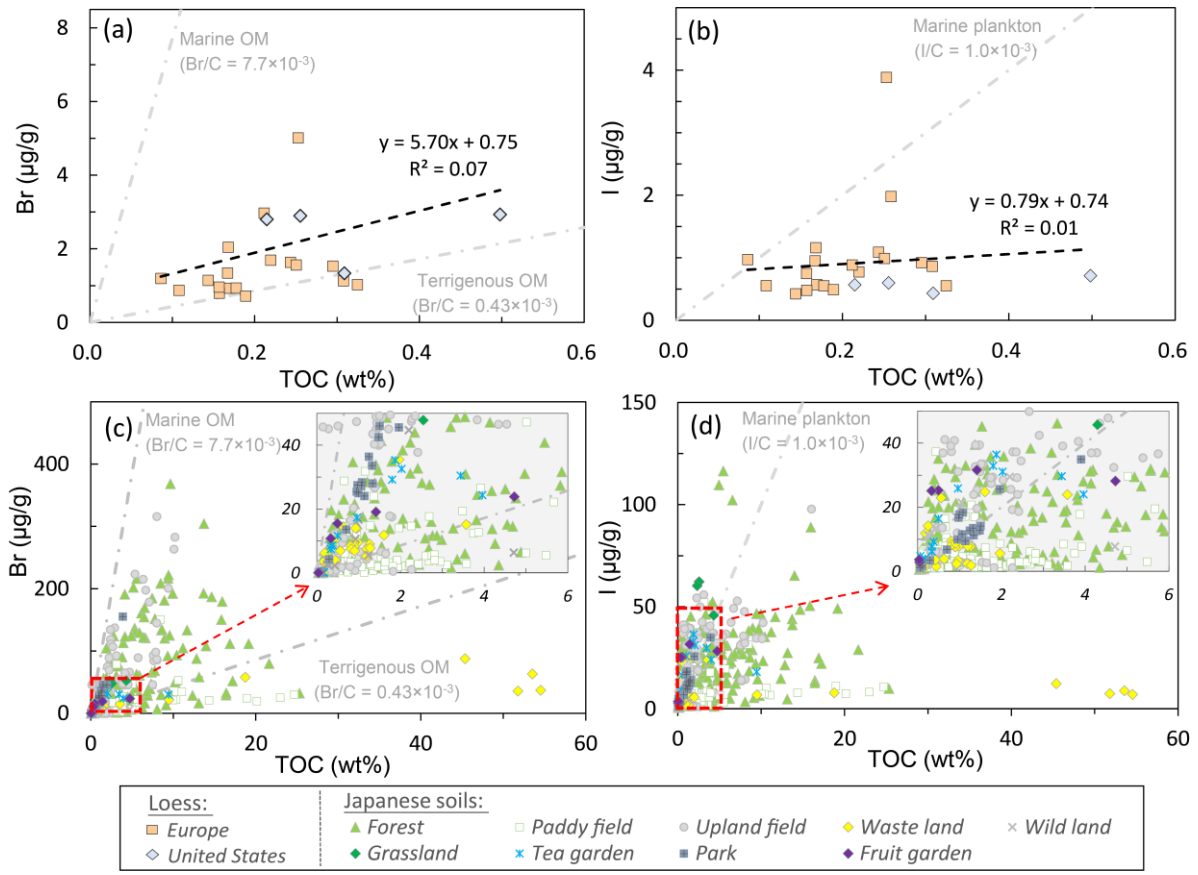

Figure S-10 Br and I versus TOC content of loess samples **(a-b**, this study**)** and Japanese soils **(c-d**, Yamasaki *et al.*, 2015**)**. In **(a)** and **(b)**, the correlation of Br and I with TOC of the analysed loess samples is indicated by the black dashed line, both showing very poor correlation (R^2 value ≤ 0.1). Br/C ratios for organic matter (OM) of terrigenous and marine sources ($0.43*10^{-3}$ and $7.7*10^{-3}$, respectively, from Mayer *et al.* (2007)) are plotted as grey dash-dotted lines in **(a)** and **(c)** for comparison. In b and d, the grey dash-dotted line represents the I/C ratio ($1.0*10^{-3}$) of typical marine plankton (Elderfield and Truesdale, 1980).

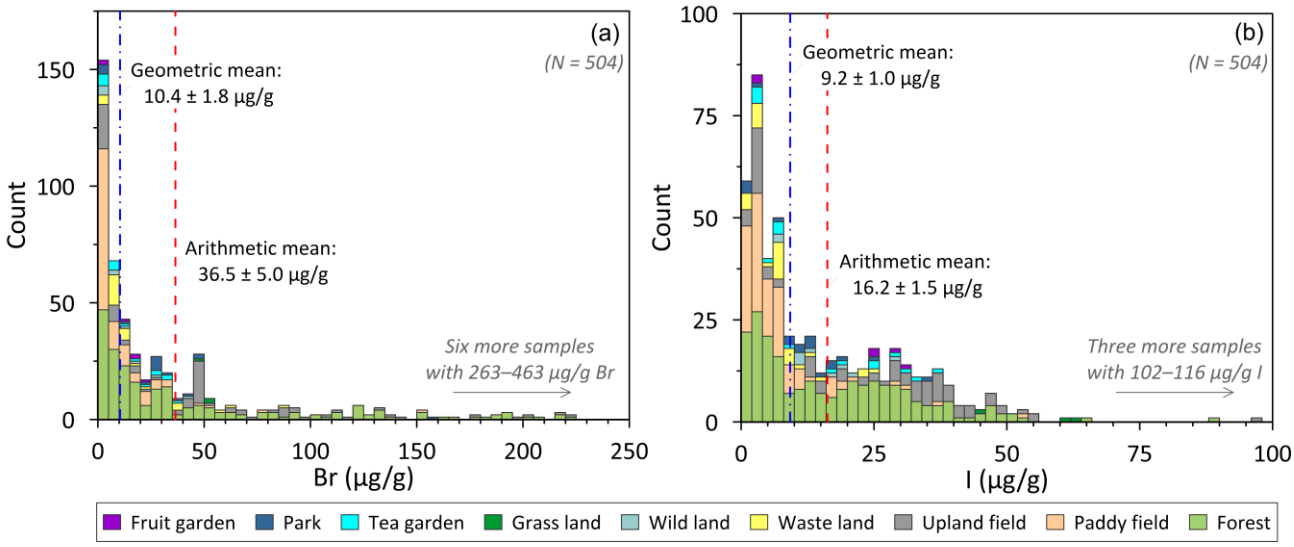

Figure S-11 Bromine and I content in various types of Japanese soil samples (Yamasaki *et al.*, 2015). The blue dash-dotted and the red dashed lines represent the geometric and arithmetic means of the dataset, respectively, along with 2 standard errors. Their calculations are the same as those for the loess data, see Figure S-5 for further details.

Supplementary Information References

Elderfield, H., Truesdale, V.W. (1980) On the biophilic nature of iodine in seawater. *Earth and Planetary Science Letters* 50, 105-114. https://doi.org/10.1016/0012-821X(80)90122-3

An, Z., Kukla, G.J., Porter, S.C., Xiao, J. (1991) Magnetic susceptibility evidence of monsoon variation on the Loess Plateau of central China during the last 130,000 years. *Quaternary Research* 36, 29-36. https://doi.org/10.1016/0033-5894(91)90015-W

Antoine, P., Rousseau, D.-D., Moine, O., Kunesch, S., Hatté, C., Lang, A., Tissoux, H., Zöller, L. (2009) Rapid and cyclic aeolian deposition during the Last Glacial in European loess: a high-resolution record from Nussloch, Germany. *Quaternary Science Reviews* 28, 2955-2973. https://doi.org/10.1016/j.quascirev.2009.08.001

Che, X., Li, G. (2013) Binary sources of loess on the Chinese Loess Plateau revealed by U–Pb ages of zircon. *Quaternary Research* 80, 545-551. https://doi.org/10.1016/j.yqres.2013.05.007

Derbyshire, E., Meng, X., Kemp, R.A. (1998) Provenance, transport and characteristics of modern aeolian dust in western Gansu Province, China, and interpretation of the Quaternary loess record. *Journal of arid environments* 39, 497-516. https://doi.org/10.1006/jare.1997.0369

Ding, Z., Ren, J., Yang, S., Liu, T. (1999) Climate instability during the penultimate glaciation: Evidence from two high-resolution loess records, China. *Journal of Geophysical Research: Solid Earth* 104, 20123-20132. https://doi.org/10.1029/1999JB900183

Feng, Z.-D., Ran, M., Yang, Q., Zhai, X., Wang, W., Zhang, X., Huang, C. (2011) Stratigraphies and chronologies of late Quaternary loess–paleosol sequences in the core area of the central Asian arid zone. *Quaternary International* 240, 156-166. https://doi.org/10.1016/j.quaint.2010.10.019

Gaschnig, R.M., Rudnick, R.L., McDonough, W.F., Kaufman, A.J., Valley, J.W., Hu, Z., Gao, S., Beck, M.L. (2016) Compositional of the upper continental crust through time, as constrained by ancient glacial diamictites. *Geochimica et Cosmochimica Acta* 186, 316-343. https://doi.org/10.1016/j.gca.2016.03.020

Greaney, A.T., Rudnick, R.L., Romaniello, S.J., Johnson, A.C., Gaschnig, R.M., Anbar, A.D. (2020) Molybdenum isotope fractionation in glacial diamictites tracks the onset of oxidative weathering of the continental crust. *Earth and Planetary Science Letters* 534, 116083. https://doi.org/10.1016/j.epsl.2020.116083

Guan, Q., Pan, B., Gao, H., Li, N., Zhang, H., Wang, J. (2008) Geochemical evidence of the Chinese loess provenance during the Late Pleistocene. *Palaeogeography, Palaeoclimatology, Palaeoecology* 270, 53-58. https://doi.org/10.1016/j.palaeo.2008.08.013

Guo, Z., Liu, T., An, Z. (1994) Paleosols of the last 0.15 Ma in the Weinan loess section and their paleoclimatic significance. *Quaternary Sciences* 14, 256-269.

Guo, Z., Biscaye, P., Wei, L., Chen, X., Peng, S., Liu, T. (2000) Summer monsoon variations over the l1.2 Ma from the weathering of loess-soil sequences in China. G*eophysical Research Letters* 27, 1751-1754. https://doi.org/10.1029/1999GL008419

Han, P.-Y., Rudnick, R.L., He, T., Marks, M.A., Wang, S.-J., Gaschnig, R.M., Hu, Z.-C. (2023) Halogen (F, Cl, Br, and I) concentrations of the upper continental crust through time as recorded in ancient glacial diamictite composites. *Geochimica et Cosmochimica Acta* 341, 28-45. https://doi.org/10.1016/j.gca.2022.11.012

He, T., Xie, J., Hu, Z., Liu, T., Zhang, W., Chen, H., Liu, Y., Zong, K., Li, M. (2018) A rapid acid digestion technique for the simultaneous determination of bromine and iodine in fifty-three Chinese soils and sediments by ICP-MS. *Geostandards and Geoanalytical Research* 42, 309-318. https://doi.org/10.1111/ggr.12212

Jahn, B.-m., Gallet, S., Han, J. (2001) Geochemistry of the Xining, Xifeng and Jixian sections, Loess Plateau of China: eolian dust provenance and paleosol evolution during the last 140 ka. *Chemical Geology* 178, 71-94. https://doi.org/10.1016/S0009-2541(00)00430-7

John, T., Scambelluri, M., Frische, M., Barnes, J.D., Bach, W. (2011) Dehydration of subducting serpentinite: implications for halogen mobility in subduction zones and the deep halogen cycle. *Earth and Planetary Science Letters* 308, 65-76. https://doi.org/10.1016/j.epsl.2011.05.038

Jovanovič, M., Gaudenyi, T., O'Hara-Dhand, K., Smalley, I. (2014) Karl Caesar von Leonhard (1779–1862), and the beginnings of loess research in the Rhine valley. *Quaternary Internationa*l 334, 4-9. https://doi.org/10.1016/j.quaint.2013.02.003

Kendrick, M.A., D'Andres, J., Holden, P., Ireland, T. (2018) Halogens (F, Cl, Br, I) in thirteen USGS, GSJ and NIST international rock and glass reference materials. *Geostandards and Geoanalytical Research* 42, 499-511. https://doi.org/10.1111/ggr.12229

Li, Y., Song, Y., Yan, L., Chen, T., An, Z. (2015) Timing and spatial distribution of loess in Xinjiang, NW China. *PLoS One* 10, e0125492. https://doi.org/10.1371/journal.pone.0125492

Marks, M.A., Kendrick, M.A., Eby, G.N., Zack, T., Wenzel, T. (2017) The F, Cl, Br and I Contents of Reference Glasses BHVO-2G, BIR-1G, BCR-2G, GSD-1G, GSE-1G, NIST SRM 610 and NIST SRM 612. *Geostandards and Geoanalytical Research* 41, 107-122. https://doi.org/10.1111/ggr.12128

Martignier, L., Nussbaumer, M., Adatte, T., Gobat, J.-M., Verrecchia, E.P. (2015) Assessment of a locally-sourced loess system in Europe: The Swiss Jura Mountains. *Aeolian Research* 18, 11-21. https://doi.org/10.1016/j.aeolia.2015.05.003

Mayer, L.M., Schick, L.L., Allison, M.A., Ruttenberg, K.C., Bentley, S.J. (2007) Marine vs. terrigenous organic matter in Louisiana coastal sediments: The uses of bromine: organic carbon ratios. *Marine Chemistry* 107, 244-254. https://doi.org/10.1016/j.marchem.2007.07.007

McLennan, S.M. (1993) Weathering and Global Denudation. *The Journal of Geology* 101, 295-303. https://doi.org/10.1086/648222

Nesbitt, H., Young, G. (1982) Early Proterozoic climates and plate motions inferred from major element chemistry of lutites. *Nature* 299, 715-717. https://doi.org/10.1038/299715a0

Park, J.-W., Hu, Z., Gao, S., Campbell, I.H., Gong, H. (2012) Platinum group element abundances in the upper continental crust revisited–New constraints from analyses of Chinese loess. *Geochimica et Cosmochimica Acta* 93, 63-76. https://doi.org/10.1016/j.gca.2012.06.026

Rodbell, D.T., Forman, S.L., Pierson, J., Lynn, W.C. (1997) Stratigraphy and chronology of Mississippi Valley loess in western Tennessee. *Geological Society of America Bulletin* 109, 1134-1148. https://doi.org/10.1130/0016-7606(1997)109%3C1134:SACOMV%3E2.3.CO;2

Sayago, J.M. (1995) The Argentine neotropical loess: an overview. *Quaternary Science Reviews* 14, 755-766. https://doi.org/10.1016/0277-3791(95)00050-X

Schellenberger, A., Veit, H. (2006) Pedostratigraphy and pedological and geochemical characterization of Las Carreras loess–paleosol sequence, Valle de Tafí, NW-Argentina. *Quaternary Science Reviews* 25, 811-831. https://doi.org/10.1016/j.quascirev.2005.07.011

Schulze, T., Schwahn, L., Fülling, A., Zeeden, C., Preusser, F., Sprafke, T. (2022) Investigating the loess–palaeosol sequence of Bahlingen-Schönenberg (Kaiserstuhl), southwestern Germany, using a multi-methodological approach. *E&G Quaternary Science Journal* 71, 145-162. https://doi.org/10.5194/egqsj-71-145-2022

Sun, D., Liu, D., Chen, M., An, Z., John, S. (1997) Magnetostratigraphy and palaeoclimate of red clay sequences from Chinese Loess Plateau. *Science in China Series D: Earth Sciences* 40, 337-343. https://doi.org/10.1007/BF02877564

Sun, D., Shaw, J., An, Z., Cheng, M., Yue, L. (1998) Magnetostratigraphy and paleoclimatic interpretation of a continuous 7.2 Ma Late Cenozoic eolian sediments from the Chinese Loess Plateau. *Geophysical Research Letters* 25, 85-88. https://doi.org/10.1029/97GL03353

Wang, H., Follmer, L.R., Liu, J.C.-l. (2000) Isotope evidence of paleo–El Niño–Southern Oscillation cycles in loess-paleosol record in the central United States. *Geology* 28, 771-774. https://doi.org/10.1130/0091-7613(2000)28<771:IEOPNO>2.0.CO;2

Xiao, G., Dai, G., Tian, S., Peng, S., Li, L., Meng, X., Yin, Q. (2023) Periodic variations of alpine glaciation and desertification of the NE Tibetan Plateau: Evidence from the loess-paleosol sequences in the Menyuan Basin. *Global and Planetary Change* 226, 104160. https://doi.org/10.1016/j.gloplacha.2023.104160

Yamasaki, S.-i., Takeda, A., Watanabe, T., Tagami, K., Uchida, S., Takata, H., Maejima, Y., Kihou, N., Tsuchiya, N. (2015) Bromine and iodine in Japanese soils determined with polarizing energy dispersive X-ray fluorescence spectrometry. *Soil Science and Plant Nutrition* 61, 751-760. https://doi.org/10.1080/00380768.2015.1054773

Yu, Y., Wang, H., Liu, X. (2012) Geochemical Characteristics of Loess Deposition since Last Interglacial at Desert Margin and Its Provenance and Climatic Implications. *Acta Sedimentologica Sinica* 30, 356-365.

Zhao, H., Lu, Y., Wang, C., Chen, J., Liu, J., Mao, H. (2010) ReOSL dating of aeolian and fluvial sediments from Nihewan Basin, northern China and its environmental application. *Quaternary Geochronology* 5, 159-163. https://doi.org/10.1016/j.quageo.2009.03.008